

Spin Domains Generate Hierarchical Ground State Structure in $J = \pm 1$ Spin Glasses

Guy Hed¹, Alexander K. Hartmann², Dietrich Stauffer³ and Eytan Domany¹

¹ Department of Physics of Complex Systems, Weizmann Institute of Science, Rehovot 76100, Israel

² Institut für Theoretische Physik, Universität Göttingen, Bunsenstr. 9, 37073 Göttingen, Germany

³ Institute for Theoretical Physics, University of Cologne, Zulpicher Straße 77, D-50937 Köln, Germany
(March 19, 2019)

Unbiased samples of ground states were generated for the short range Ising spin glass with $J_{ij} = \pm 1$, in three dimensions. Clustering the ground states revealed their hierarchical organization; cluster analysis of the spins unraveled the existence of highly correlated domains. The structure of the ground states is explained in terms of the spin domains' relative orientation.

PACS numbers: 75.10.Nr, 75.50.Lk, 05.50+q, 75.40.Mg

Whereas equilibrium properties of infinite range [1] spin glasses (SG) are completely understood within the framework of replica symmetry breaking (RSB) [2], SG with short range interactions are the subject of current debate and controversy [3-5]. Open questions address the nature of the low temperature phases [2,6] and their theoretical description [6,3,7-9]. Resolution of these issues by experiments or simulations is hindered by the extremely long relaxation time required for equilibration.

The model: We study the ground states (GS) of the Edwards-Anderson model [10] of an Ising spin glass

$$H = \sum_{\langle ij \rangle} J_{ij} S_i S_j; \quad J_{ij} = \pm 1 \quad (1)$$

where $\langle ij \rangle$ denotes nearest neighbor sites of a cubic lattice; the values $J_{ij} = \pm 1$ are assigned to each bond independently and with equal probabilities [11]. This model is very special - it has highly degenerate [12] GS. Nevertheless, we expect that its low temperature ($T > 0$) properties are generic, i.e. not qualitatively different from other J_{ij} distributions (such as Gaussian). On the other hand, the low- T properties of the model (1) are most probably dominated by the structure of its GS. Hence we hope that the GS of the $J = \pm 1$ model provide insight about the low- T behavior of generic short range Ising SG. Irrespective of the validity of this hope, the GS structure of this model is interesting on its own merit.

We study this model because there exist efficient algorithms [13] to produce ground states. We extended these to generate unbiased samples of the GS; i.e. we "equilibrated" our system at $T = 0$. We studied the GS of the model (1) with periodic boundary conditions in $d = 2; 3; 4$ dimensions, with $N = L^d$ spins, for several sizes L . For each d and L up to 1000 realizations fJg were produced; for each realization an unbiased sample of M GS has been generated and analyzed (M few thousand). We discuss here $d = 3$; see [14] for $d = 2; 4$.

Summary of the main results: 1. For a given realization fJg , the GS do not cover the hypercube $S = (S_1; S_2; \dots; S_N)$ uniformly; rather, there is a hierarchical structure to the GS, as shown schematically in Fig. 1 and in detail in 3. The set of all GS splits into two clusters C and \bar{C} , related by spin reversal; C splits into C_1 and C_2 , and so on.

2. There exist contiguous spin domains that are correlated over the GS. The largest two spin clusters, G_1 and G_2 contain $O(N)$ spins, typically with $|G_1| \approx 5|G_2|$.

3. The structure of the GS is explained in terms of these spin domains. In the states of C_1 , both G_1 and G_2 are frozen, into states denoted in Fig. 1 as $\backslash*$. When passing from a state in C_1 to one in C_2 the smaller cluster, G_2 is flipped; when going from C_1 to \bar{C}_1 , both spin clusters are reversed (see Fig. 1). In any particular GS, however, a spin domain is not free to flip on its own, only together with some of the spins at its boundaries.

4. This picture, of state partitions governed by the states of correlated spin domains of decreasing sizes [14], is our model for the hierarchical organization of the $T = 0$ pure states and their spatial structure; it may be the short-range version of RSB. Our data indicate [14] that these pure states do not have an ultrametric structure.

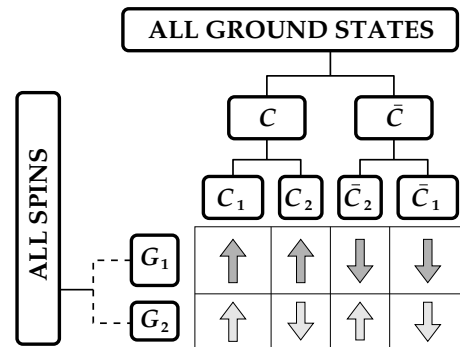


FIG. 1. Schematic representation of our picture; the two largest spin domains and the first two levels in the hierarchical organization of the GS are shown. The structure of the GS is explained by the spin domains' orientations; e.g. in the GS of the two sets $C_1; C_2$, the spins of G_1 have the same orientation, whereas the spins of the smaller cluster, G_2 , have flipped.

We explain now how this picture of GS structure and spin clusters has been found; we present evidence that substantiates our findings, investigate their dependence on system size and discuss their implications.

Generating unbiased samples of ground states: For ev-

ery realization $fJ_{ij}g$ we used the genetic cluster exact approximation (CEA) algorithm [13] to sample the GS. The GS generated this way were divided into valleys [15]; a valley V consists of all the GS that can be traversed by flipping one spin at a time without changing the energy. By performing zero temperature Monte-Carlo simulations [14], starting from initial states provided by the CEA, we are able to generate an unbiased sample of the states within each valley. Samples of GS produced by the CEA are, however, biased: small valleys are over-represented [16] and we do not know $\langle j \rangle$; the correct number of GS in each valley.

For realizations with less than 10^6 GS we overcame this by obtaining all GS and selecting M of these at random. When the number of GS is large we use a new form of an empirical scaling relation [17], based on local measurements of $n_r(\cdot)$, the number of GS in V that differ from a GS by less than r spins. We found that

$$\frac{\ln n_r}{\ln \langle j \rangle} = 1 - a \exp\left(-b + c \ln N\right) \frac{r \ln r}{\ln \langle j \rangle} \quad (2)$$

with $a = 0.325$, $b = 0.492$ and $c = 0.124$. n_r is the average of $n_r(\cdot)$ over a sample of g V .

By fitting n_r to the form of (2), we estimate $\langle j \rangle$; Fig 2 shows the extent to which (2) holds. Using $\langle j \rangle$ we generate our sample of M GS, in which each valley has its proper weight. These M GS have the form of an $N \times M$

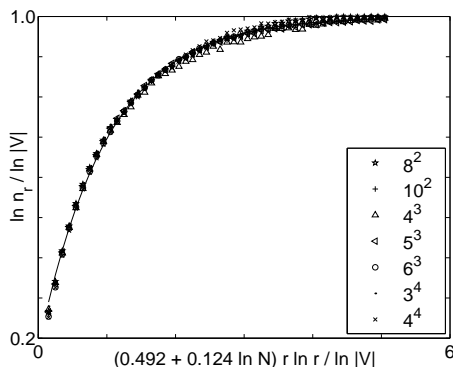


FIG. 2. Testing the scaling relation (2). Only those realizations, for which exact enumeration of the GS has been performed, were used. Each point is the average of a bin of size 0.1; data were collected from all the valleys and all the realizations used. Valleys of less than 20 ground states were excluded. The error bars are smaller than the symbol sizes.

table of binary valued entries, $S_i = \pm 1; i = 1; \dots; N; = 1; \dots; M$, which serves as the input of cluster analysis.

Clustering methodology: Clustering is a powerful way to perform exploratory analysis of all kinds of data. In general, one has the coordinates of n points, calculates a distance matrix between pairs of points and determines the underlying hierarchy of partitions (clusters) in the data. We used Ward's agglomerative algorithm [18]; it starts with each data point as a separate cluster and at

each step fuses the pair of clusters c_i, c_j that are at the shortest effective distance [18]

from each other, stopping when all points are in one cluster.

Ward's algorithm tries, in effect, to minimize the sum of squared distances within each cluster. We associate a value d_{ij} with each cluster c_i , where $d_{ij} = d_{ji}$ is the effective distance between the two clusters that were fused to form c_i . This value is related to d_{ij} . For the initial single state clusters we set $d_{ij} = 0$. Clusters formed earlier have lower d_{ij} values. The algorithm produces a dendrogram such as Fig. 3 (a). Leaves represent individual data points; they are ordered horizontally in a way that reflects their proximity in the dendrogram [19]. The boxes at the nodes represent clusters; their vertical coordinates are their d_{ij} values. The length of the branch above a cluster provides a measure of its relative value.

We analyzed the data in two ways: 1. viewing the GS as M data-points and 2. viewing the spins as N data-point. The two ways were coupled [20] to interpret the GS in terms of spin domains.

Clustering the Ground States: Each GS of our sample is represented by a vector $S = (S_1; S_2; \dots; S_N)$. The distance D between any pair of GS is

$$D = \frac{1}{2} \sqrt{\frac{1}{2N} \sum_{i=1}^N S_i^2 S_i^2} \quad (3)$$

The dendrogram obtained by clustering $M = 500$ GS for a system with $N = 6^3$ spins is shown in Fig 3 (a). The hierarchical GS structure sketched in Fig. 1 is evident. In general, for our system sizes we could study in detail partitions into C, C , and their sub-partitions into C_1, C_2, C_1 and C_2 . For this particular realization fJg the partition of C_1 into two subclusters is also well defined.

Ordering the GS according to the results of the clustering procedure, we get the distance matrix D shown in Fig 3 (b); dark represents short distances and light-high. The structure of the GS, as read from the dendrogram, is clearly seen, and is even more striking when the 500 GS are projected onto the 2 or 3 dimensional subspace spanned by the principal components [14].

In order to understand this hierarchical structure of the GS we turn to investigate the manner in which the N spins are organized in the M GS.

Clustering the spins: Every spin i is represented as an M -component vector $S_i = (S_i^1; S_i^2; \dots; S_i^M)$. To identify domains of spins that are correlated over our sample of M states we measure

$$C_{ij} = \frac{1}{M} \sum_{k=1}^M S_i^k S_j^k \quad (4)$$

Since in a spin glass the gauge dependent sign of C_{ij} has no significance, the proper distance of two spins is

$$d_{ij} = \sqrt{1 - C_{ij}^2} \quad (5)$$

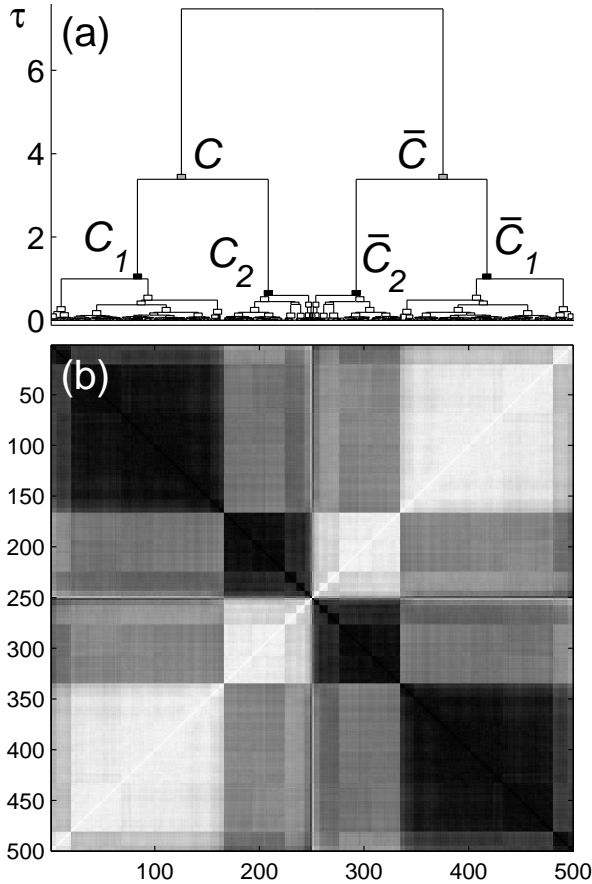


FIG. 3. (a) The dendrogram obtained by clustering the ground states, for a particular set of J_{ij} , for $N = 6^3$ spins. (b) When the states are ordered according to the dendrogram, a clear block structure is seen in D , the distance matrix of the G.S. Darker shades correspond to shorter distances.

A typical outcome of clustering the spins with this distance matrix is the dendrogram D of Fig. 4 (a), obtained for the same system of 6^3 spins, whose GS were studied above. We also show, in Fig. 4 (b), the distance matrix with the spins reordered according to D . Evidently there is non-trivial structure in the spin-space, in terms of which we now interpret the GS hierarchy.

Spin clusters explain the ground states' structure: For each realization fJg we obtained such a pair of dendrograms, one describing the GS and one for the spins. We were able to identify in the spin dendrogram SD two (or more) large clusters $G_1;G_2$ that form highly correlated contiguous spin domains. In terms of these we were able to interpret the GS structure, in accordance with the picture sketched in Fig. 1. Identification of $G_1;G_2$ is not simple; we may have spins that are fixed in states from C_1 but not fixed in C_2 and vice versa. We overcame this problem by clustering GS and spins in a coupled way [20]. For example, in the case shown in Fig. 4, we indicate two spin clusters, g_1 and g_2 , which serve as candidates for playing the roles of G_1 and G_2 . Details of how these

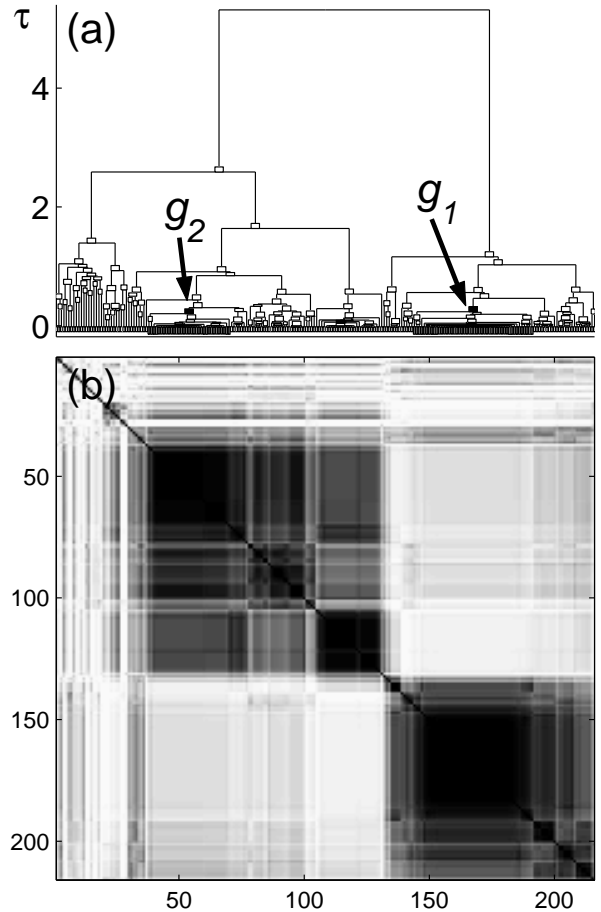


FIG. 4. (a) The dendrogram D obtained by clustering the spins of the system of Fig. 3. The best candidates for the two largest correlated domains are marked as g_1 and g_2 . (b) When the spins are ordered according to the dendrogram, a structure of correlated spin domains emerges; darker shades correspond to shorter distances and higher correlations.

candidates are identified and selected will be given elsewhere [14]. Here we only show that our identification indeed yielded spin clusters whose size scales as the system size and which indeed explain the GS structure in the way sketched in Fig. 1.

Testing the validity of the picture: According to our picture we expect $|g_{ij}|/L^d$ for both $i=1;2$. We present the distributions of $|g_{ij}|/L^3$ for $4 \leq L \leq 8$ in Fig. 5 (a). They are broad for both $i=1;2$; that of G_1 peaks at 0.9, with mean 0.75 and standard deviation 0.18; the numbers for the smaller cluster are 0.05 (peak), 0.11 (mean value) and 0.11 (s.d.). The distributions for $L=4$ differ somewhat from those for $L=5;6;8$ whereas the latter three seem to be very close to one another, indicating that the L -dependence of these size distributions may have converged already for $L=8$ [14]. Our results show that the sizes of the two largest spin clusters do scale as L^3 .

We turn to present a figure of merit which measure quantitatively the extent to which $G_1;G_2$ and $C_1;C_2$ in-

indeed conform to the picture of Fig. 1.

The squared correlation of two spins, $i \in G_1$ and $j \in G_2$, averaged over all such pairs is

$$C_{12}^2 = \frac{1}{\sum_{i \in G_1} \sum_{j \in G_2}} \sum_{i \in G_1} \sum_{j \in G_2} C_{ij}^2 \quad (6)$$

In the "ideal" situation our picture holds for all states from C_1 and C_2 and for all such pairs of spins, and then

$$C_{12}^2 = C_{12}^{2, \text{ideal}} = \frac{\sum_{i \in G_1} \sum_{j \in G_2} C_{ij}^2}{\sum_{i \in G_1} \sum_{j \in G_2} 1} \quad (7)$$

The average distance between two GS, $2 \in C_1$, $2 \in C_2$, is

$$D_{12} = \frac{1}{\sum_{i \in G_1} \sum_{j \in G_2}} \sum_{i \in G_1} \sum_{j \in G_2} D_{ij} \quad (8)$$

In the ideal situation we have $D_{12} = D_{12}^{\text{ideal}} = \frac{1}{\sum_{i \in G_1} \sum_{j \in G_2}} \sum_{i \in G_1} \sum_{j \in G_2} D_{ij} = \frac{1}{2N} \sum_{i \in G_1} \sum_{j \in G_2} D_{ij}$. Our figure of merit I is defined by

$$I = \frac{1}{2} \left(C_{12}^2 - C_{12}^{2, \text{ideal}} \right)^2 + D_{12} - D_{12}^{\text{ideal}} \quad (9)$$

If the behavior of the system conforms to our picture, the distribution of I conforms to $\delta(I)$. As can be seen in Fig. 5(b), the distribution indeed becomes sharper and closer to a delta function as the system size increases. This indicates that our picture of two macroscopic correlated spin domains governing the structure of the first two GS clusters is indeed correct and deviations from it have lower statistical weight as the system size increases.

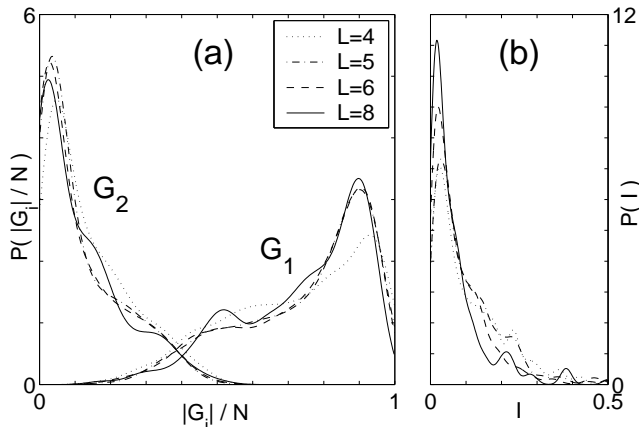


FIG. 5. (a) Size distributions of G_1 and G_2 for three-dimensional systems of various sizes. (b) The distribution of I for the same systems.

Ultrametricity, $P(q)$: We measured the commonly studied [4,5] distribution function $P(q)$ for the overlap between pure states at $T=0$ and found functions that look very much like those measured at low T for larger systems with Gaussian interactions [7]. We believe that our picture explains also the pure states found there, supporting our expectation that our findings, obtained for $J_{ij} = 1$, have general relevance.

We investigated ultrametricity of our set of GS. Ultrametricity implies that every triangle composed of three pure states (i.e. the average or centroid of a valley V of states) is either equilateral or isosceles, with $d_{12} = d_{13} = d_{23}$. We tested ultrametricity by picking three valleys (all from C_1), constructing a triangle (in state space), identifying the longest side d_{12} and the shortest d_{13} , and measuring $R = [d_{12} - d_{13}] / d_{12}$. Ultrametricity implies that the distribution of (R) approaches $\delta(R)$; we find [14] that it approaches a distribution with mean 0.77 and s.d. 0.30, clearly violating ultrametricity.

Summary: The ground states of the short-range Ising spin glass have a hierarchical, tree-like structure. The state clusters can be understood in terms of the behavior of correlated contiguous spin domains. When we pass from one state-cluster to another, some spin domains are flipped. This structure of GS and the associated barriers is, to a large extent, consistent with the RSB based picture, but without ultrametricity.

We thank the Germany-Israel Science Foundation for support, I. Kanter and M. Mezard for helpful discussions, and N. Jan for hospitality to D.S.

Electronic address: Guy.Hed@weizmann.ac.il

- [1] D. Sherrington and S. Kirkpatrick, Phys. Rev. Lett. 35, 1792 (1975).
- [2] M. Mezard, G. Parisi, N. Sourlas, G. Toulouse and M. A. Virasoro, J. Phys. 45, 843 (1984).
- [3] M. A. Moore, H. Bokil and B. Drossel, Phys. Rev. Lett. 81, 4252 (1998).
- [4] M. Palassini and A. P. Young, Phys. Rev. Lett. 83, 5126 (1999).
- [5] S. Franz and G. Parisi, cond-mat/0006188 (2000).
- [6] D. S. Fisher and D. A. Huse, Phys. Rev. B 38, 386 (1988).
- [7] E. Marinari, G. Parisi and J. J. Ruiz-Lorenzo, Phys. Rev. B, 58, 852 (1998).
- [8] J. Houdayer and O. C. Martin, Europhys. Lett. 49, 794 (2000).
- [9] S. Franz and F. Ricci-Tersenghi, Phys. Rev. E 61, 1121 (2000).
- [10] S. F. Edwards and P. W. Anderson, J. Phys. F 5, 965 (1975).
- [11] In fact we ensured to have equal numbers of positive and negative bonds.
- [12] S. Kirkpatrick, Phys. Rev. B 16, 4630 (1977).
- [13] A. K. Hartmann, Physica A 224, 480 (1996); Phys. Rev. E 59, 84 (1999).
- [14] G. Hed, E. Domany, A. K. Hartmann and D. Stauer, unpublished.
- [15] A. K. Hartmann, J. Phys. A 33, 657 (2000).
- [16] A. K. Hartmann, Physica A 275, 1 (1999).
- [17] A. K. Hartmann, Eur. Phys. J. B 13, 591 (2000).
- [18] A. K. Jain and R. C. Dubes, Algorithms for Clustering Data, Prentice-Hall, Englewood Cliffs (1988).

- [19] U. Alon, N. Barkai, D. A. Notterman, K. Gish, S. Ybarra, D. Mack and A. J. Levine, PNAS 96, 6745 (1999).
- [20] G. Getz, E. Levine and E. Domany, unpublished.